

---

**MAGNETISM  
AND FERROELECTRICITY**

---

## **XAFS Studies of the Local Environment of Pb Impurity Atoms in Barium, Strontium, and Calcium Titanates**

**A. I. Lebedev<sup>a</sup>, I. A. Sluchinskaya<sup>a</sup>, A. Erko<sup>b</sup>, A. A. Veligzhanin<sup>c</sup>, and A. A. Chernyshov<sup>c</sup>**

<sup>a</sup> *Moscow State University, Moscow, 119991 Russia*

*e-mail: swan@scon155.phys.msu.su*

<sup>b</sup> *BESSY GmbH, Berlin, 12489 Germany*

<sup>c</sup> *Russian Research Centre Kurchatov Institute, pl. Kurchatova 1, Moscow, 123182 Russia*

Received August 21, 2008

**Abstract**—The local environment of Pb impurity atoms in BaTiO<sub>3</sub>, SrTiO<sub>3</sub>, and CaTiO<sub>3</sub> crystals was studied by XAFS technique. It is shown that, in both polar and nonpolar phases of BaTiO<sub>3</sub> and in SrTiO<sub>3</sub>, the Pb atoms are displaced from the *A* lattice sites by ~0.15 Å; in CaTiO<sub>3</sub> this displacement is absent. Large values of Debye–Waller factors (0.05–0.10 Å<sup>2</sup>) for the atoms in the first shell of Pb observed in all the three crystals indicate the distortion of the oxygen environment of Pb atoms. The appearance of these features was explained by the fact that the Pb–O chemical bond has a noticeable covalent component and a Pb atom can form strong bonds only with four of the 12 surrounding oxygen atoms. The obtained data were used to determine the main factors responsible for the occurrence of ferroelectric phase transition in SrTiO<sub>3</sub> and CaTiO<sub>3</sub> and for the increase of the Curie temperature of BaTiO<sub>3</sub> when it is doped with Pb.

PACS numbers: 61.10.Ht, 61.72.Dd, 77.84.Dy

DOI: 10.1134/S1063783409050175

### 1. INTRODUCTION

Ferroelectrics with a perovskite structure  $ABO_3$  are widely used in modern electronics. As known, the replacement of atoms in these crystals significantly influences the ferroelectric phase transition temperature  $T_c$  and may cause the appearance of ferroelectricity in incipient ferroelectrics like SrTiO<sub>3</sub> [1]. Optimization of the properties of solid solutions of ferroelectrics is closely related to the understanding of the origin of phase transitions (PTs) occurring in them. However, in spite of a large volume of experimental data, there are a number of unsolved problems related, in particular, to understanding of the microscopic mechanisms of the influence of impurities on the PTs in solid solutions of perovskites.

XAFS (X-ray absorption fine structure) spectroscopy is one of the modern powerful methods of studying the material structure at a microscopic level. The studies of perovskites by this method have revealed earlier unknown specific features of their local structure which are important for understanding the mechanisms of PTs occurring in them [2–10]. However, the only SrTiO<sub>3</sub>-based solid solution studied by XAFS spectroscopy was solid solution Sr<sub>1-x</sub>Ba<sub>x</sub>TiO<sub>3</sub> [10]. It is hoped that XAFS studies of strontium titanate crystals doped with various impurities will help in elucidating the mechanism of ferroelectricity in these materials.

At present, solid solutions based on BaTiO<sub>3</sub>, SrTiO<sub>3</sub>, and CaTiO<sub>3</sub> with a Pb impurity are used to develop

piezoelectric devices and nonlinear elements of microwave engineering. However, from the fundamental standpoint, the Pb impurity in titanates with a perovskite structure is an interesting object of study owing to its electronic structure [11]. From the data available in the literature, it is known that the introduction of lead into BaTiO<sub>3</sub>, SrTiO<sub>3</sub>, and CaTiO<sub>3</sub> increases the PT temperatures. However, it is unclear why lead is the only impurity increasing the PT temperature in BaTiO<sub>3</sub> among various impurities whose atomic radii are smaller than that of barium [12].

In this work, we study the local environment of lead impurity atoms in barium, strontium, and calcium titanates using XAFS spectroscopy. The results of studying these three matrices in combination with the data available in the literature on the influence of lead impurity on the lattice parameter and the PT temperature allow us to determine the main factors responsible for the increased PT temperature in crystals doped with lead.

### 2. EXPERIMENTAL

The extended X-ray-absorption fine-structure (EXAFS) and X-ray-absorption near-edge structure (XANES) studies were conducted on the BESSY synchrotron radiation source (the beam energy, 1.7 GeV; maximum beam current, 290 mA) on the station KMC-2 and on the Siberia-2 synchrotron radiation source (the beam energy, 2.5 GeV; maximum beam current, 100 mA) at the Kurchatov Center for Synchrotron

Radiation (on the station SAS). The preliminary measurements of the spectra were carried out on the station SAS equipped with a Si(111) channel-cut monochromator; the spectra were recorded by two scintillation detectors measuring the intensity of scattering by a foil of a beam incident on the sample (with intensity  $I_0$ ) and the intensity of the sample fluorescence radiation  $I_f$ . The measurements were performed at the Pb  $L_{III}$  edge (13.055 keV) and Sr  $K$  edge (16.105 keV) at 300 K.

More detailed measurements were carried out at BESSY, where radiation was monochromatized by a double-crystal monochromator made of  $\text{Si}_{1-x}\text{Ge}_x$  with the (111) orientation. The radiation intensity incident on the sample was measured by an ionization chamber, and the fluorescence radiation intensity was measured by a  $p$ - $i$ - $n$  diode. In addition to the measurements of the EXAFS spectra of  $\text{Ba}_{1-x}\text{Pb}_x\text{TiO}_3$  samples at the Pb  $L_{III}$  edge at 300 K, the temperature dependence of the EXAFS spectra was measured on heating up to a temperature of 490 K, which exceeds the ferroelectric PT temperature of the crystal. These measurements were carried out in a high-temperature chamber with a beryllium window. Moreover, the XANES at the Ti  $K$  edge (4.966 keV) was studied at BESSY at 300 K, with the titanium fluorescence radiation being detected using a silicon drift detector operating in an energy-dispersive regime.

The  $\text{Ba}_{1-x}\text{Pb}_x\text{TiO}_3$  ( $x = 0.05, 0.10$ ),  $\text{Sr}_{1-x}\text{Pb}_x\text{TiO}_3$  ( $x = 0.02, 0.20$ ), and  $\text{Ca}_{1-x}\text{Pb}_x\text{TiO}_3$  ( $x = 0.1, 0.2$ ) samples studied were obtained by the oxalate method [13] based on codeposition of low-soluble double salts  $(\text{Ba,Sr,Ca})[\text{TiO}](\text{C}_2\text{O}_4)_2 \cdot n\text{H}_2\text{O}$  from aqueous solutions. The starting components were  $\text{K}_2[\text{TiO}](\text{C}_2\text{O}_4)_2 \cdot 2\text{H}_2\text{O}$ , nitrates of barium, calcium, and strontium, and  $\text{Pb}(\text{CH}_3\text{COO})_2 \cdot \text{H}_2\text{O}$  of the ChDA or KhCh grade. The obtained sediment was annealed in air in a closed alumina crucible in a furnace at a temperature of 540–750°C for 2 to 72 h. An advantage of the oxalate method is the possibility of preparing samples with an exact stoichiometric composition at a low temperature, which is particularly important when operating with such a volatile impurity as Pb.

The lead concentration in the samples was chosen according to the phase diagrams of the  $\text{SrTiO}_3$ ( $\text{CaTiO}_3$ ,  $\text{BaTiO}_3$ )– $\text{PbTiO}_3$  systems [11, 12]. The chosen solid-solution compositions satisfy the requirement that the solid solutions be in a nonpolar phase at 300 K. An exception is barium titanate-based solid solutions, which are ferroelectric at room temperature over the entire Pb concentration range.

X-ray diffraction was used to control whether the samples are single-phase. The obtained samples are nanocrystalline powders, with coherent scattering domains being  $\sim 250$  Å in size. The small size of the crystallites leads to broadening of all reflections, which hampers the exact determination of the lattice parameters. Nevertheless, from the character of the splitting

and broadening of the reflections, we concluded that  $\text{Ca}_{0.8}\text{Pb}_{0.2}\text{TiO}_3$ ,  $\text{Ba}_{0.9}\text{Pb}_{0.1}\text{TiO}_3$ , and  $\text{Sr}_{0.8}\text{Pb}_{0.2}\text{TiO}_3$  are in the orthorhombic ( $a = 5.576$  Å,  $b = 7.836$  Å,  $c = 5.503$  Å), tetragonal ( $\bar{a} = 3.999$  Å), and cubic ( $a = 3.912$  Å) phases, respectively.

The EXAFS function was extracted from the fluorescence excitation spectra  $\mu(E) = I_f/I_0$  (where  $E$  is the X-ray photon energy) by the traditional method [14]. After subtracting the background below the absorption edge, we extracted, using splines, the smooth part  $\mu_0(E)$  of the spectrum and calculated the dependence of  $\chi = (\mu - \mu_0)/\mu_0$  on the photoelectron wave vector  $k = [2m(E - E_0)/\hbar^2]^{1/2}$ . The reference energy  $E_0$  is taken to be the energy of the inflection point of the  $\mu(E)$  curve. For each sample, two to four spectra were measured, which were then processed independently and the obtained  $\chi(k)$  dependences were averaged. From the obtained  $\chi(k)$  curves, information was extracted concerning the first two coordination shells using the direct and inverse Fourier transforms with a modified Hamming window. By fitting the calculated spectrum

$$\chi(k) = \frac{(-1)^l}{k} \sum_j \frac{S_0^2 N_j}{R_j^2} f(k, \pi) \times \exp\left(-\frac{2R_j}{\lambda(k)} - 2k^2 \sigma_j^2\right) \sin[2kR_j + 2\delta_l(k) + \phi_j(k)]$$

to an experimental curve (least square technique, the weighting factor  $k^2$ ), we found the distances  $R_j$  and the Debye–Waller factors  $\sigma_j^2$  for each of the coordination shells ( $j = 1, 2$ ) and also the correction  $dE_0$  to the reference energy. The coordination numbers  $N_j$  were taken to be those known for the perovskite structure. The quantity  $S_0^2$  which takes into account many-electron effects and inelastic scattering was a fitting parameter. The orbital angular momentum  $l$  is determined by the absorption edge ( $l = 0$  for the  $K$  edge and  $l = 1$  for the  $L$  edge). The theoretical dependences of the backscattering amplitude  $f(k, \pi)$ , scattering phase  $\phi_j(k)$ , photoelectron escape phase  $\delta_l(k)$ , and mean free path  $\lambda(k)$  were calculated using the FEFF software package [15]. The total number of adjustable parameters was 6, and the number of independent parameters in the data was  $N_{\text{ind}} = 2\Delta k \Delta R / \pi = 12$ –16.

### 3. RESULTS

The experimental  $k^2\chi(k)$  dependences and their best fits obtained for  $\text{Ba}_{0.9}\text{Pb}_{0.1}\text{TiO}_3$ ,  $\text{Sr}_{0.8}\text{Pb}_{0.2}\text{TiO}_3$ , and  $\text{Ca}_{0.8}\text{Pb}_{0.2}\text{TiO}_3$  samples are shown in Figs. 1–3.

An analysis of these data shows that the local environment of Pb atoms in different matrices are qualitatively similar. A comparison of the measured spectra with the spectra calculated under the assumption that the Pb atoms substitute for atoms either in sites  $A$  or in

sites  $B$  shows that the Pb atoms are in the  $A$  sites. In all the three systems studied, the EXAFS signal is mainly formed by atoms in the second coordination shell (Ti) located at a distance of 3.31–3.46 Å, while the signal from the nearest neighboring oxygen atoms in the first coordination shell ( $R \sim 2.7$  Å) is strongly suppressed (the Debye–Waller factor  $\sigma_1^2 = 0.05$ – $0.10$  Å<sup>2</sup> is unexpectedly high when compared to the value  $0.01$  Å<sup>2</sup> characteristic of other oxides).

The small difference between the distances to the first and second coordination shells in the perovskite structure makes their separation upon the Fourier filtration in the  $R$  space impossible, and the data for the third coordination shell are strongly distorted by multiple scattering. The splitting of the distances to all coordination shells caused by possible displacements of the Pb atoms from the lattice sites may increase the number of adjustable parameters necessary to describe a distorted structure, and this number may become larger than that of the independent parameters ( $N_{\text{ind}}$ ) in the data. Because of this, we quantitatively determine the structural parameters restricting ourselves to the two nearest coordination shells and analyzing the data within the models in which local distortions of the structure are described by a minimum number of parameters.

Lest the number of the adjustable parameters increase, when analyzing the data for  $\text{Ca}_{1-x}\text{Pb}_x\text{TiO}_3$  and  $\text{Ba}_{1-x}\text{Pb}_x\text{TiO}_3$ , we assumed lattice distortions (orthorhombic or tetragonal) to be small and used simplified models in which the lattice is cubic.

One of such models for quantitative determination of local distortions is a model in which the Pb atoms are displaced along the fourfold axis and the other atoms are in fixed positions. An analysis of the data in terms of this model (see table) shows small displacements of the lead atoms from their lattice sites in  $\text{Sr}_{1-x}\text{Pb}_x\text{TiO}_3$  and  $\text{Ba}_{1-x}\text{Pb}_x\text{TiO}_3$  and unusually high Debye–Waller thermal factors for the Pb–O bonds (obtained after subtracting the static Debye–Waller factor associated with the displacement of a Pb atom from its site) in all the three systems studied. In calcium titanate, no displacement of the Pb atoms was observed. The Pb atom shift from a site in  $\text{Ba}_{1-x}\text{Pb}_x\text{TiO}_3$  is no surprise, since the samples are in the ferroelectric phase at 300 K. However, this shift is also retained on heating of the samples above the PT temperature. Thus, the obtained results indicate that the Pb atoms are off-center in  $\text{SrTiO}_3$  and  $\text{BaTiO}_3$ . For  $\text{BaTiO}_3$ , this conclusion is confirmed by the fact that the displacement of the Pb atoms with respect to the Ti atoms in the polar phase (0.14 Å) is approximately threefold greater than that of Ba atoms with respect to Ti in undoped  $\text{BaTiO}_3$  [12]. A drawback of the model under discussion is that it does not explain anomalously large Debye–Waller thermal factor for the first coordination shell (Pb–O).

We also considered a model in which the Pb and Ti atoms can be displaced independently along a fourfold

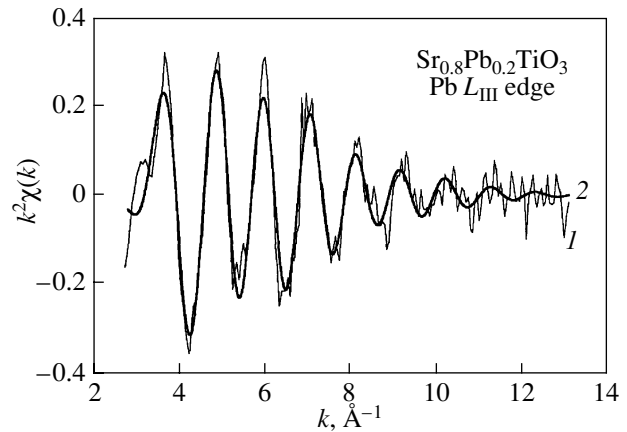


Fig. 1. (1) Experimental dependence of  $k^2\chi$  on  $k$  for  $\text{Sr}_{0.8}\text{Pb}_{0.2}\text{TiO}_3$  and (2) its best theoretical fit.

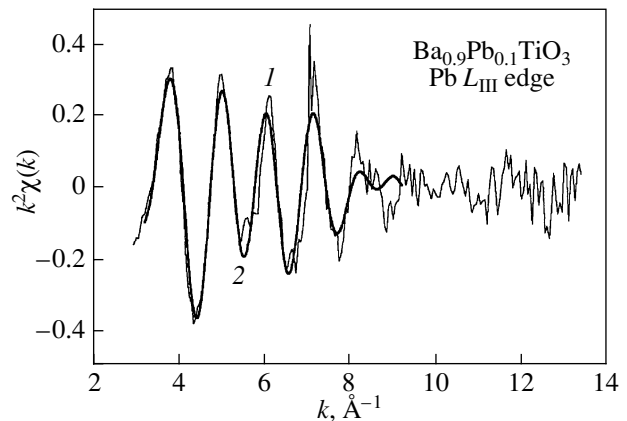


Fig. 2. (1) Experimental dependence of  $k^2\chi$  on  $k$  for  $\text{Ba}_{0.9}\text{Pb}_{0.1}\text{TiO}_3$  and (2) its best theoretical fit.

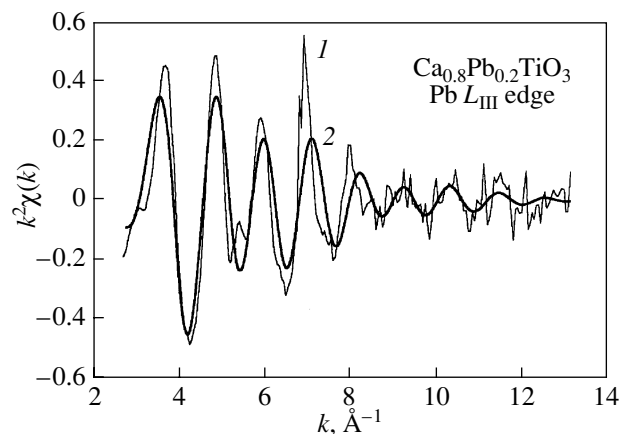


Fig. 3. (1) Experimental dependence of  $k^2\chi$  on  $k$  for  $\text{Ca}_{0.8}\text{Pb}_{0.2}\text{TiO}_3$  and (2) its best theoretical fit.

Structure parameters obtained from processing the EXAFS data in terms of three models ( $i = 1, 2$  are the coordination shell numbers)

Structural parameters	Sample					
	$\text{Ba}_{1-x}\text{Pb}_x\text{TiO}_3$ ( $x = 0.05, 0.10$ )		$\text{Sr}_{0.8}\text{Pb}_{0.2}\text{TiO}_3$		$\text{Ca}_{0.8}\text{Pb}_{0.2}\text{TiO}_3$	
	$R_i, \text{\AA}$	$\sigma_i^2, \text{\AA}^2$	$R_i, \text{\AA}$	$\sigma_i^2, \text{\AA}^2$	$R_i, \text{\AA}$	$\sigma_i^2, \text{\AA}^2$
Model 1						
1 (Pb–O)	2.82	0.16	2.76	0.11–0.13	2.70	0.12
2 (Pb–Ti)	3.46	0.009	3.39	0.002–0.005	3.31	0.019
Pb displacement	0.145		0.13–0.14		0	
Model 2						
1 (Pb–O)	2.82	0.019	2.76	0.022	2.70	0.014
2 (Pb–Ti)	3.46	0.009	3.39	0.009	3.31	0.016
Pb displacement	0.42–0.46		0.40		0.40	
Ti displacement	0.27–0.32		0.28		0.40	
Model 3						
1 (Pb–O)	2.82	0.008–0.011	2.76	0.016	2.70	0.015
2 (Pb–Ti)	3.46	0.012–0.041	3.39	0.011	3.31	0.014
Pb displacement	~0.06		0.09		0	
Rotation angle, deg	13		12		12	

axis, with the positions of the oxygen atoms being fixed. The results of analyzing the data in terms of this model are given in the table. It follows from the table that the displacement of Pb atoms with respect to the Ti atoms in  $\text{Sr}_{1-x}\text{Pb}_x\text{TiO}_3$  and  $\text{Ba}_{1-x}\text{Pb}_x\text{TiO}_3$  is 0.12–0.15 Å; i.e., it is the same as in the first model. In  $\text{Ca}_{1-x}\text{Pb}_x\text{TiO}_3$ , the Pb atoms are not displaced with respect to the Ti atoms within the limits of experimental error. In this case, good agreement between the calcu-

lated and experimental spectra is achieved when the Pb and Ti atoms are shifted from their sites by 0.3–0.4 Å.

The large shift of the Ti atoms with respect to the oxygen atoms obtained in the second model must be manifested in the XANES spectra at the Ti  $K$  edge, because the intensity of the near-edge peak related to  $1s \rightarrow 3d(e_g)$  transitions of the Ti atom forbidden in the dipole approximation is very sensitive to the shift of this atom from the center of the oxygen octahedron [16]. For this reason, we studied these spectra.

The XANES spectra recorded at the Ti  $K$  edge are shown in Fig. 4. It is seen that, in  $\text{SrTiO}_3$  and  $\text{BaTiO}_3$ , the intensity of the  $1s \rightarrow 3d(e_g)$  transition at an energy of 4969 eV remains practically unchanged as Pb is partially substituted for Sr and Ba, although the intensity of this peak in  $\text{BaTiO}_3$  is markedly higher than that in  $\text{SrTiO}_3$ . The absence of an influence of the lead impurity on the intensity of the  $1s \rightarrow 3d(e_g)$  transition demonstrates that the Pb doping of the crystal is not accompanied by an increase in the Ti atom displacement from the center of the oxygen octahedron. The higher intensity of these transitions in  $\text{BaTiO}_3$  is due to the fact that, at 300 K, the sample is in the ferroelectric phase, in which Ti atoms are slightly shifted from the octahedron center and a noticeable contribution from the oxygen  $2p$  states arises in the final state of these optical transitions.

It is interesting that the intense peak of  $1s \rightarrow 3d$  transitions is also characteristic of  $\text{Ca}_{1-x}\text{Pb}_x\text{TiO}_3$ , while

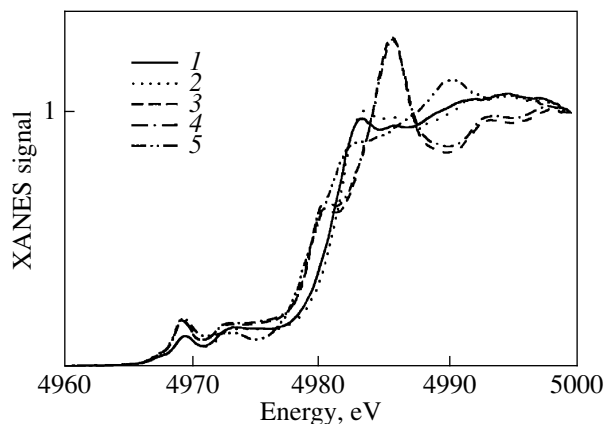


**Fig. 4.** XANES spectra measured at the Ti  $K$  edge for (1)  $\text{Sr}_{0.8}\text{Pb}_{0.2}\text{TiO}_3$ , (2)  $\text{Sr}_{0.98}\text{Pb}_{0.02}\text{TiO}_3$ , (3)  $\text{Ba}_{0.95}\text{Pb}_{0.05}\text{TiO}_3$ , (4)  $\text{Ba}_{0.9}\text{Pb}_{0.1}\text{TiO}_3$ , and (5)  $\text{Ca}_{0.8}\text{Pb}_{0.2}\text{TiO}_3$ .

the undoped calcium titanate undergoes only a structural PT accompanied by a rotation and small deformation of the oxygen octahedra, with the titanium remaining in the centrosymmetric position. We assume that this may be related either to the existence of a local disorder in  $\text{Ca}_{1-x}\text{Pb}_x\text{TiO}_3$ , which is manifested in the occurrence of first-order Raman scattering in the cubic phase [17], or to the presence in our samples of some fraction of an amorphous phase characterized by the existence of four- and fivefold coordinated titanium [18].

The conclusion that the displacement of Ti from the center of the oxygen octahedron is insignificant according to the XANES data does not agree with the large displacement of the Ti atom obtained in the second model. Because of this, we considered a third model taking into account a possible rotation of the oxygen octahedra.

The third model assumes a possibility of simultaneous displacements of the Pb atoms from their sites along a fourfold axis and the rotation of the oxygen octahedra with fixed positions of the titanium atoms. We assumed that the rotation of the oxygen octahedra is similar to that in the low-temperature phase of  $\text{SrTiO}_3$ . As the rotation of the oxygen octahedra during the high-temperature structural PT in  $\text{CaTiO}_3$  is more complex than that in  $\text{SrTiO}_3$ , the parameters obtained for  $\text{CaTiO}_3$  in this model may only qualitatively characterize the magnitude of distortions. The results of analyzing the EXAFS spectra in terms of the third model are given in the table. As follows from the table, the Pb atoms in  $\text{Sr}_{1-x}\text{Pb}_x\text{TiO}_3$  and  $\text{Ba}_{1-x}\text{Pb}_x\text{TiO}_3$  are shifted from their lattice sites; however, the shifts are somewhat smaller than those in the first and second models. In  $\text{CaTiO}_3$ , within the accuracy of experiment, the Pb atoms are not displaced. Unlike the second model, the third model does not contradict the results of analyzing the XANES data. As for the values of the rotation angles, they agree with the data available in the literature only for  $\text{CaTiO}_3$ . In  $\text{SrTiO}_3$ , they exceed the experimentally observed angles by a factor of  $\sim 6$ . In  $\text{BaTiO}_3$ , the rotations must be absent at all (there is no structural PT).

Note that the above models used to quantitatively analyze distortions of the local structure include only the simplest and evident distortions. Real distortions can be more complex; in particular, they can include the lattice relaxation around an impurity atom and the deformation of the oxygen octahedra. However, in this case, the number of adjustable parameters increases significantly and their values cannot be determined from the EXAFS data. Nevertheless, the models considered above allow one to estimate possible various distortions of the local structure in the solid solutions and draw certain conclusions concerning the reasons of the ferroelectric PTs in  $\text{SrTiO}_3$  and  $\text{CaTiO}_3$  and the increase in  $T_c$  in  $\text{BaTiO}_3$  doped with lead.

#### 4. DISCUSSION OF THE RESULTS

The properties of an isovalent impurity substituting for A atoms in the lattice differ from those of the substituted atoms. First, the impurity deforms the lattice around it and changes the crystal lattice parameter. Second, the electronic characteristics of the substituting and substituted atoms (polarizability, electronegativity, etc.) are different. Third, the chemical bond between an impurity atom and its local environment can differ in character from the chemical bond in the host lattice. Each of these factors can influence the conditions of the occurrence of ferroelectricity and the PT temperature in a doped crystal.

Let us compare our results with the known data on the influence of the Pb impurity on  $T_c$  in the three matrices under consideration. As is known from the data available in the literature [1, 11, 12], the Pb doping of these three matrices increases the Curie temperature. The doping of  $\text{BaTiO}_3$  decreases its lattice parameter, and doping of  $\text{SrTiO}_3$  and  $\text{CaTiO}_3$  increases their lattice parameters.

Consider the influence of the first ("size") factor mentioned above on the ferroelectric PT temperature. The influence of a doping-induced change in the lattice parameter on  $T_c$  can be considered, in a first approximation, as the effect of a uniform compression or stretching of the host matrix. Since a compression of a crystal usually decreases the ferroelectric PT temperature, the doping of a crystal by atoms larger than the substituted atoms must increase  $T_c$  and the doping by smaller atoms must decrease  $T_c$ . Since the  $\text{Pb}^{2+}$  ionic radius is smaller than the  $\text{Ba}^{2+}$  radius, the decrease in the lattice parameter of  $\text{BaTiO}_3$  doped with lead must decrease the Curie temperature. This conclusion contradicts the fact that the experimentally measured  $T_c$  of  $\text{BaTiO}_3$  increases with lead doping [12]. On the other hand, our experimental data indicate that lead atoms occupy off-center positions in  $\text{BaTiO}_3$ . Thus, it is reasonable to conclude that the increase in  $T_c$  of the solid solution  $\text{Ba}_{1-x}\text{Pb}_x\text{TiO}_3$  is caused by the off-centering of the lead atoms, which compensates the decrease in the PT temperature due to the size factor.

In  $\text{SrTiO}_3$ , the ionic radius of  $\text{Sr}^{2+}$  is smaller than that of  $\text{Pb}^{2+}$ . Therefore, according to the size effect under discussion, the Curie temperature must increase with lead doping. Our experimental data indicate that lead ions occupy off-center positions in  $\text{SrTiO}_3$ . Because of this, we cannot unambiguously conclude which of these two factors (size effect or off-centering) determines the increase in  $T_c$  of  $\text{SrTiO}_3$  doped with lead.

In our experiments, we did not observe off-center lead atoms in calcium titanate. This is likely due to the fact that Pb atoms are strongly "clamped" in the lattice. Since the ionic radius of  $\text{Pb}^{2+}$  is markedly larger than that of  $\text{Ca}^{2+}$  and the Pb ions do not occupy off-center positions, the increase in  $T_c$  of  $\text{CaTiO}_3$  doped with lead

can be explained only by an increase in the lattice parameter.

Aside from the shift of Pb atoms from *A* sites, our experiments revealed unusually large values of the Debye–Waller factor for the Pb–O bond in all the three matrices. This might be expected in  $\text{CaTiO}_3$  and  $\text{SrTiO}_3$ , in which, as the temperature decreases, a structural PT occurs associated with the rotation of the oxygen octahedra (at 300 K, calcium titanate is already in the orthorhombic phase, and strontium titanate at this temperature can undergo large thermal fluctuations associated with the soft mode at the *R* point of the Brillouin zone). As mentioned above, the rotation angles obtained from analyzing the data agree with the data available in the literature only for  $\text{CaTiO}_3$ . In  $\text{SrTiO}_3$ , they are much greater than the angles found in other experiments.

It is the most difficult to explain the high value of the Debye–Waller factor in doped  $\text{BaTiO}_3$ , since barium titanate does not exhibit instability of the phonon spectrum at the *R* point of the Brillouin zone. The explanation of the large Debye–Waller factor in terms of the displacement of titanium ions from the octahedron centers (in the second model), as mentioned above, contradicts the XANES data. Therefore, apart from the octahedron rotation, there is another reason for the strong distortion of the oxygen environment of a lead atom in  $\text{BaTiO}_3$  and  $\text{SrTiO}_3$ .

In our opinion, the large Debye–Waller factor in  $\text{Ba}_{1-x}\text{Pb}_x\text{TiO}_3$  may be due to the deformation of octahedra caused by lead doping because the Pb–O chemical bond is predominantly covalent [19]. A Pb atom in the *A* site cannot form equivalent covalent bonds with all the oxygen atoms surrounding it. In oxygen compounds of divalent lead, the characteristic number of Pb–O bonds is equal to 4; therefore, the displacement of a lead atom from its site with the formation of covalent bonds with four of the 12 surrounding oxygen atoms can be energetically favorable. This fact explains both the off-centering of lead atoms and the strong distortion of the Pb–O bond length. These reasonings can also be used to explain the overestimated values of the Debye–Waller factor for the Pb–O bond in  $\text{Sr}_{1-x}\text{Pb}_x\text{TiO}_3$ .

Thus, from the above discussion of the causes of off-centering of atoms, we can conclude that, in addition to the difference between the sizes of substituting and substituted atoms, the change in the character of the chemical bond between an impurity atom and its nearest environment can be a more important factor causing the appearance of off-center atoms. This change can lead to the appearance of off-center impurity atoms even when their size exceeds that of the substituted atoms (the case of Pb in  $\text{SrTiO}_3$  and of Pb and Sn in GeTe [20]).

Note that, in this mechanism, the off-center Pb atom cannot be considered to be independent of its environ-

ment since, as the atom is displaced from its site as a result of the formation of a covalent bond, the oxygen atoms are also substantially displaced. This displacement is likely the reason for the large increase in the Debye–Waller factor in the crystals under consideration (in this situation, the displacement of an off-center atom cannot be determined from analyzing the EXAFS data for the first coordination shell). One would expect that, due to the displacement of the oxygen atoms, the dipole moment of the  $\text{PbO}_{12}$  cluster will be significant even for a small observed shift of the lead atom with respect to the titanium atom (0.15 Å).

The obtained results permit us to understand the microscopic mechanism of influence of the lead impurity on the ferroelectric PT in the three titanates. In  $\text{CaTiO}_3$ , a lead atom is strongly clamped in the lattice and the main effect determining the increase in the temperature  $T_c$  on doping can be only a change of the phonon spectrum (a decrease in the soft-mode frequency as a result of an increase in the lattice parameter). In contrast, in  $\text{BaTiO}_3$ , a decrease in the lattice parameter on Pb doping excludes the contribution of the size factor and the increase in  $T_c$  observed in the experiment can be explained only by the Pb off-centering. In this case, the increase in  $T_c$  can be explained as a result of the correlated motion of the dipole moments of the  $\text{PbO}_{12}$  and  $\text{TiO}_6$  clusters. The dipole moments of these clusters are parallel, since, according to the XANES data, the displacement of Ti ions in the oxygen octahedra remains unchanged. Strontium titanate is an intermediate case, since both the increase in the lattice parameter on doping and the off-centering of the lead ions in this material favor an increase in  $T_c$  observed experimentally.

## 5. CONCLUSIONS

The local environment of the lead impurity in  $\text{BaTiO}_3$ ,  $\text{SrTiO}_3$ , and  $\text{CaTiO}_3$  crystals has been studied by XAFS spectroscopy. In  $\text{BaTiO}_3$  in both the polar and nonpolar phases and in  $\text{SrTiO}_3$ , the Pb atoms are displaced from the *A* lattice sites by  $\sim 0.15$  Å; in  $\text{CaTiO}_3$ , the Pb atoms are not displaced. Unusually high values of the Debye–Waller factor for the atoms in the first coordination shell of lead (0.05–0.10 Å) observed in these three crystals are indicative of a distortion of the oxygen environment of the Pb atoms, which is due to deformation and rotations of the  $\text{TiO}_6$  octahedra.

In our opinion, the formation of the Pb–O chemical bond, which has a noticeable covalent component, is the reason for the off-centering of Pb and strong distortion of its nearest environment. The main factors responsible for the appearance of ferroelectricity and for the increase in the temperature of ferroelectric phase transition in lead-doped perovskites are the size factor in  $\text{CaTiO}_3$  and the off-center positions of Pb

atoms in BaTiO<sub>3</sub>; SrTiO<sub>3</sub> can be considered as an intermediate case.

#### ACKNOWLEDGMENTS

The authors are grateful to V.V. Mishchenko for the assistance in preparing the samples, S.G. Dorofeev for fabricating the high-temperature chamber, V.F. Kozlovskii for the assistance in performing the X-ray diffraction measurements, and the Russian–Germany Laboratory (RGL) for financial support during the measurements at BESSY.

This work was supported by the Russian Foundation for Basic Research, project no. 08-02-01436.

#### REFERENCES

1. V. V. Lemanov, *Ferroelectrics* **226**, 133 (1999).
2. O. Hanske-Petitpierre, Y. Yacoby, J. Mustre de Leon, E. A. Stern, and J. J. Rehr, *Phys. Rev. B: Condens. Matter* **44**, 6700 (1991).
3. N. Sicron, B. Ravel, Y. Yacoby, E. A. Stern, F. Dogan, and J. J. Rehr, *Phys. Rev. B: Condens. Matter* **50**, 13168 (1994).
4. A. I. Frenkel, F. M. Wang, S. Kelly, R. Ingalls, D. Haskel, E. A. Stern, and Y. Yacoby, *Phys. Rev. B: Condens. Matter* **56**, 10 869 (1997).
5. V. A. Shuvaeva, D. Zekria, A. M. Glazer, Q. Jiang, S. M. Weber, P. Bhattacharya, and P. A. Thomas, *Phys. Rev. B: Condens. Matter* **71**, 174 114 (2005).
6. R. V. Vedrinskii, E. S. Nazarenko, M. P. Lemeshko, V. Nassif, O. Proux, A. A. Novakovich, and Y. Joly, *Phys. Rev. B: Condens. Matter* **73**, 134 109 (2006).
7. M. P. Lemeshko, E. S. Nazarenko, A. A. Gonchar, L. A. Reznichenko, T. I. Nedoseykina, A. A. Novakovich, O. Mathon, Y. Joly, and R. V. Vedrinskii, *Phys. Rev. B: Condens. Matter* **76**, 134 106 (2007).
8. D. Cao, I.-K. Jeong, R. H. Heffner, T. Darling, J.-K. Lee, F. Bridges, J.-S. Park, and K.-S. Hong, *Phys. Rev. B: Condens. Matter* **70**, 224 102 (2004).
9. N. Jaouen, A. C. Dhaussy, J. P. Itié, A. Rogalev, S. Marinell, and Y. Joly, *Phys. Rev. B: Condens. Matter* **75**, 224 115 (2007).
10. V. Shuvaeva, Y. Azuma, K. Yagi, H. Terauchi, R. Vedrinskii, V. Komarov, and H. Kasatani, *Phys. Rev. B: Condens. Matter* **62**, 2969 (2000).
11. V. V. Lemanov, E. P. Smirnova, and E. A. Tarakanov, *Fiz. Tverd. Tela (St. Petersburg)* **39** (4), 714 (1997) [*Phys. Solid State* **39** (4), 628 (1997)].
12. F. Iona and G. Shirane, *Ferroelectric Crystals* (Pergamon, Oxford, 1962; Mir, Moscow, 1965).
13. W. S. Clabaugh, E. M. Swiggard, and R. Gilchrist, *J. Res. Natl. Bur. Stand. (US)* **56**, 289 (1956).
14. A. I. Lebedev, I. A. Sluchinskaya, V. N. Demin, and I. Manro, *Izv. Akad. Nauk, Ser. Fiz.* **60** (10), 46 (1996).
15. J. Mustre de Leon, J. J. Rehr, S. I. Zabinsky, and R. C. Albers, *Phys. Rev. B: Condens. Matter* **44**, 4146 (1991).
16. R. V. Vedrinskii, V. L. Kraizman, A. A. Novakovich, Ph. V. Demekhin, and S. V. Urazhdin, *J. Phys.: Condens. Matter* **10**, 9561 (1998).
17. V. M. Naik, D. Haddad, R. Naik, J. Mantese, N. W. Schurbring, A. L. Micheli, and G. W. Auner, *J. Appl. Phys.* **93**, 1731 (2003).
18. F. Farges, *Am. Mineral.* **82**, 36 (1997).
19. R. E. Cohen, *Nature (London)* **358**, 136 (1992).
20. A. I. Lebedev, I. A. Sluchinskaya, V. N. Demin, and I. H. Munro, *Pis'ma Zh. Éksp. Teor. Fiz.* **63** (8), 600 (1996) [*JETP Lett.* **63** (8), 635 (1996)].

*Translated by Yu. Ryzhkov*